SUPPORTING INFORMATION

Supplemental Figures

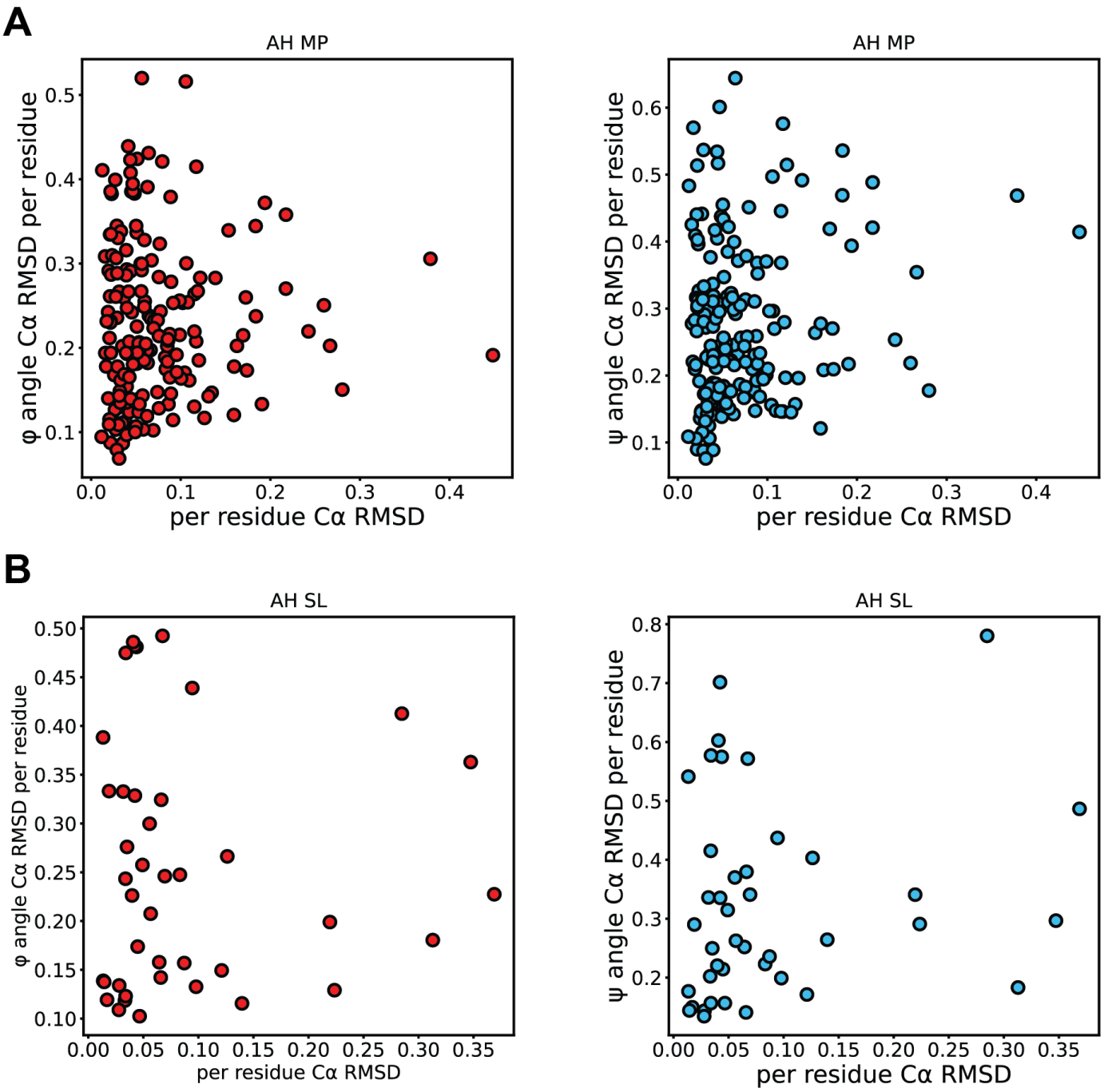

Supplemental Figure S1. Φ/Ψ angle RMSD versus normalized Cα RMSD for alpha helical peptides, **Related to Figure 2. A.** Φ (red) and Ψ (blue) angle RMSD plotted against the Cα RMSD per residue for each alpha helical membrane peptide (AH MP) in our benchmark set. **B.** Φ (red) and Ψ (blue) angle RMSD plotted against the Cα RMSD per residue for each alpha helical soluble (AH SL) peptide in our benchmark set. Φ/Ψ RMSD and Cα RMSD was calculated pairwise for all 5 AF2 models compared to each model in the NMR ensemble. The minimum RMSD among pairwise comparisons was plotted.

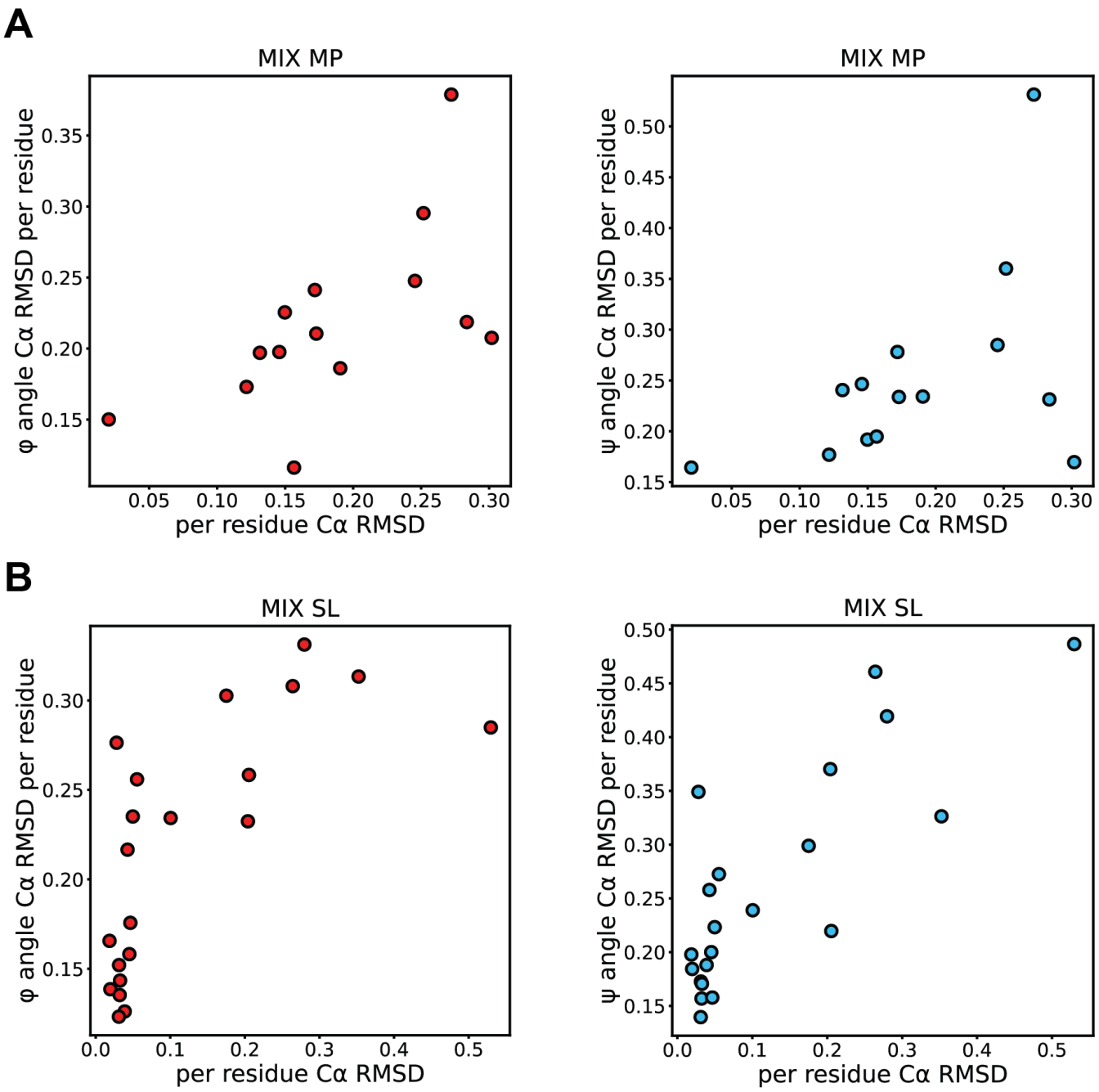

Supplemental Figure S2. Φ/Ψ angle RMSD versus normalized Cα RMSD for mixed secondary structure peptides, **Related to Figure 3**. **A.** Φ (red) and Ψ (blue) angle RMSD plotted against the Cα RMSD per residue for each mixed secondary structure membrane peptide (MIX MP) in our benchmark set. **B.** Φ (red) and Ψ (blue) angle RMSD plotted against the Cα RMSD per residue for each mixed secondary structure soluble (MIX SL) peptide in our benchmark set. Φ/Ψ RMSD and Cα RMSD was calculated pairwise for all 5 AF2 models compared to each model in the NMR ensemble. The minimum RMSD among pairwise comparisons was plotted.

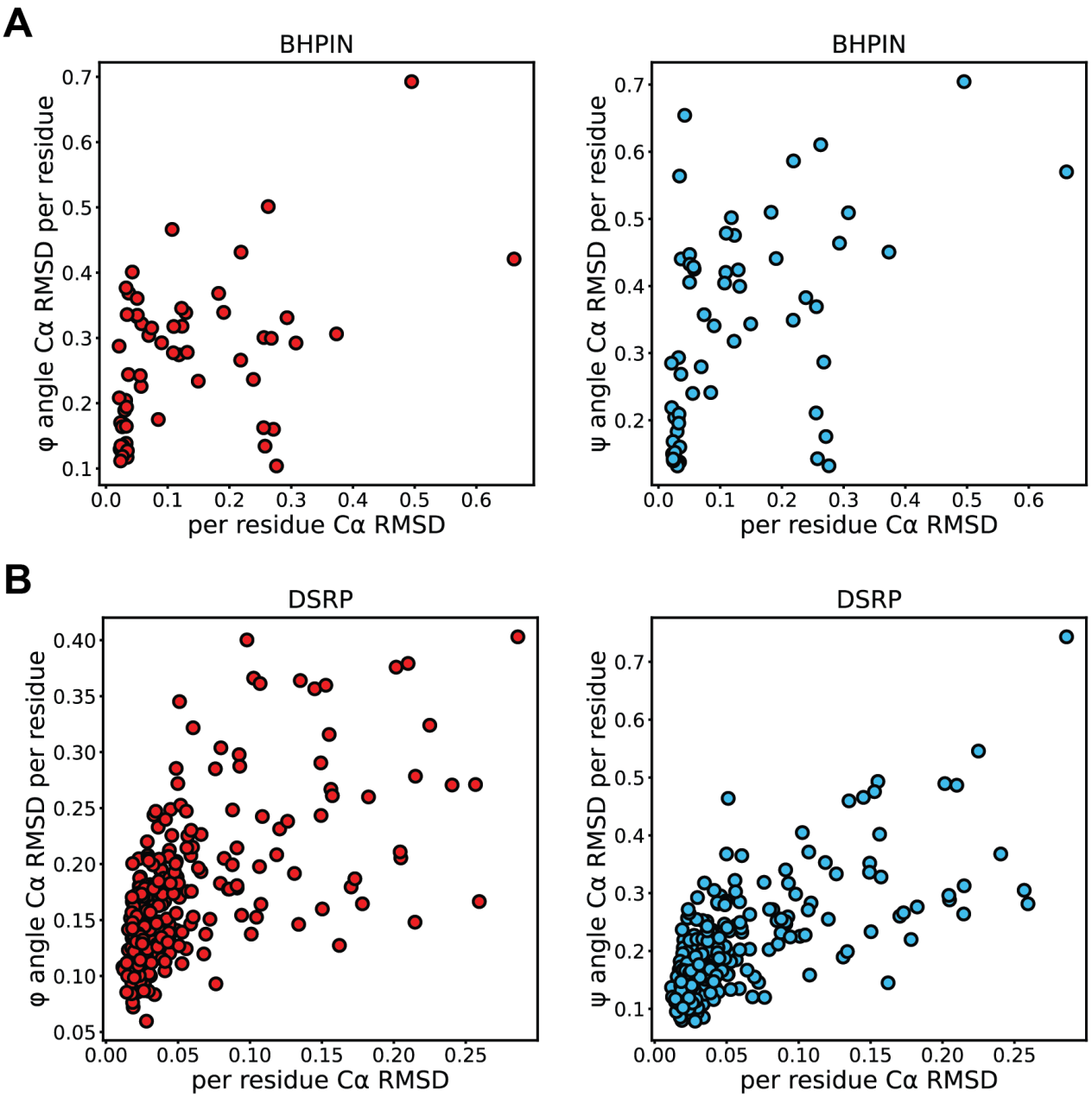

Supplemental Figure S3. Φ/Ψ angle RMSD versus normalized Cα RMSD for β-hairpin and disulfide rich peptides, Related to Figure 4. A. Φ (red) and Ψ (blue) angle RMSD plotted against the Cα RMSD per residue for each β-hairpin peptide (BHPIN) in our benchmark set. **B.** Φ (red) and Ψ (blue) angle RMSD plotted against the Cα RMSD per residue for each disulfide rich peptide (DSRP) in our benchmark set. Φ/Ψ RMSD and Cα RMSD was calculated pairwise for all 5 AF2 models compared to each model in the NMR ensemble. The minimum RMSD among pairwise comparisons was plotted.

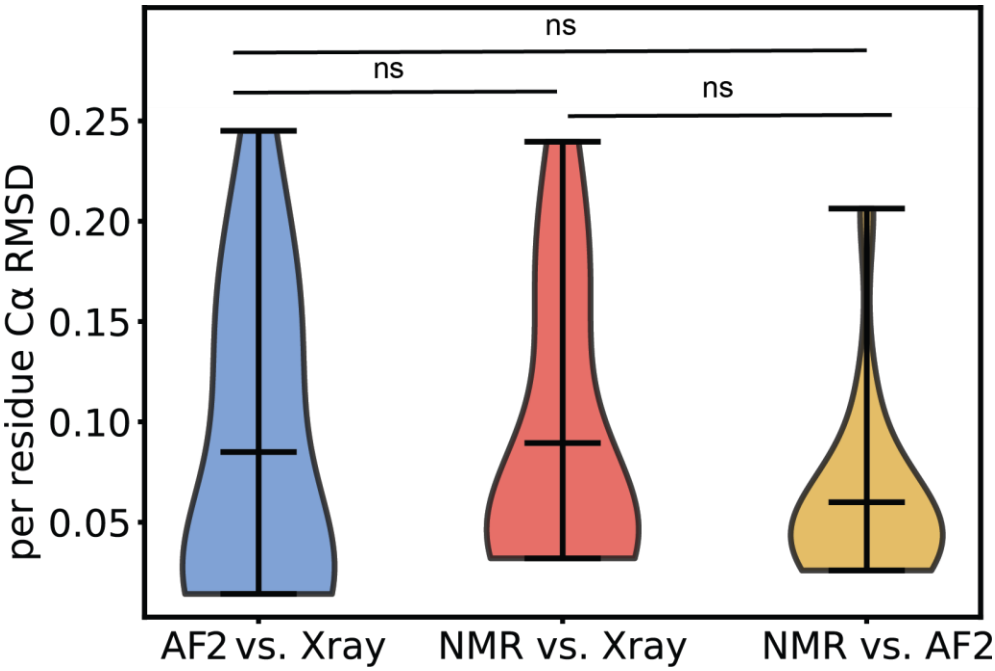

Supplemental Figure S4. X-ray models versus AlphaFold2 compared to NMR models versus AlphaFold2, Related to Star Methods. There was not a statistically significant difference between AF2's ability to predict NMR vs. Xray crystal structures. Surprisingly, NMR/X-ray RMSD comparisons failed to demonstrate lower RMSD than AF2 vs. either method, demonstrating the draw backs of both experimental and computational techniques.

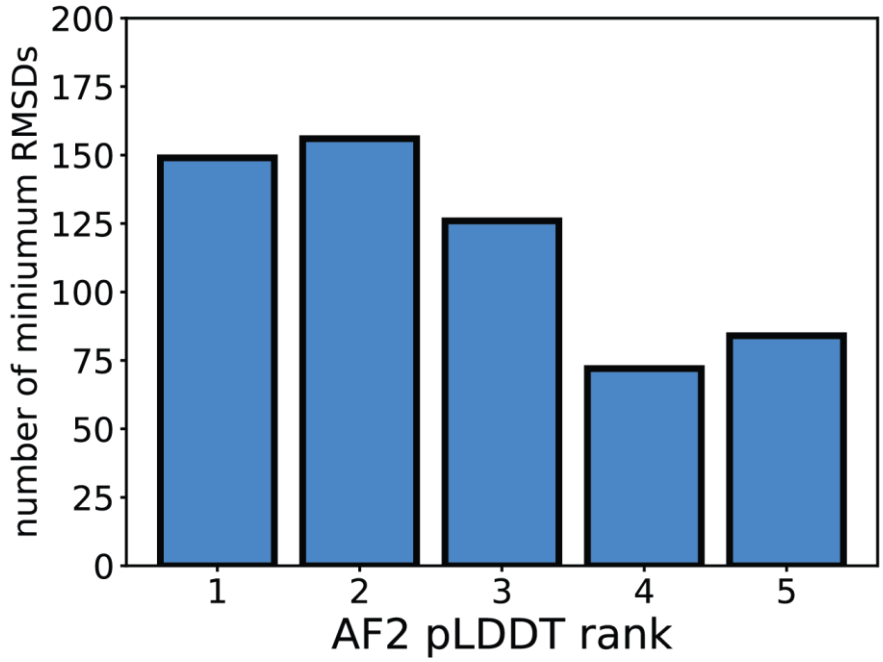

Supplemental Figure S5. Number of lowest RMSD model pairs by pLDDT ranking, Related to Star Methods. AF2 ranks structures by backbone pLDDT. We enumerated the number of rank 1, rank 2 etc. by pLDDT AF2 models for each lowest RMSD NMR model/AF2 model pairwise comparison in our benchmark set. This bar graph showed rank 1-3 models are more likely to predict NMR models than rank 4 and 5 AF2 models.

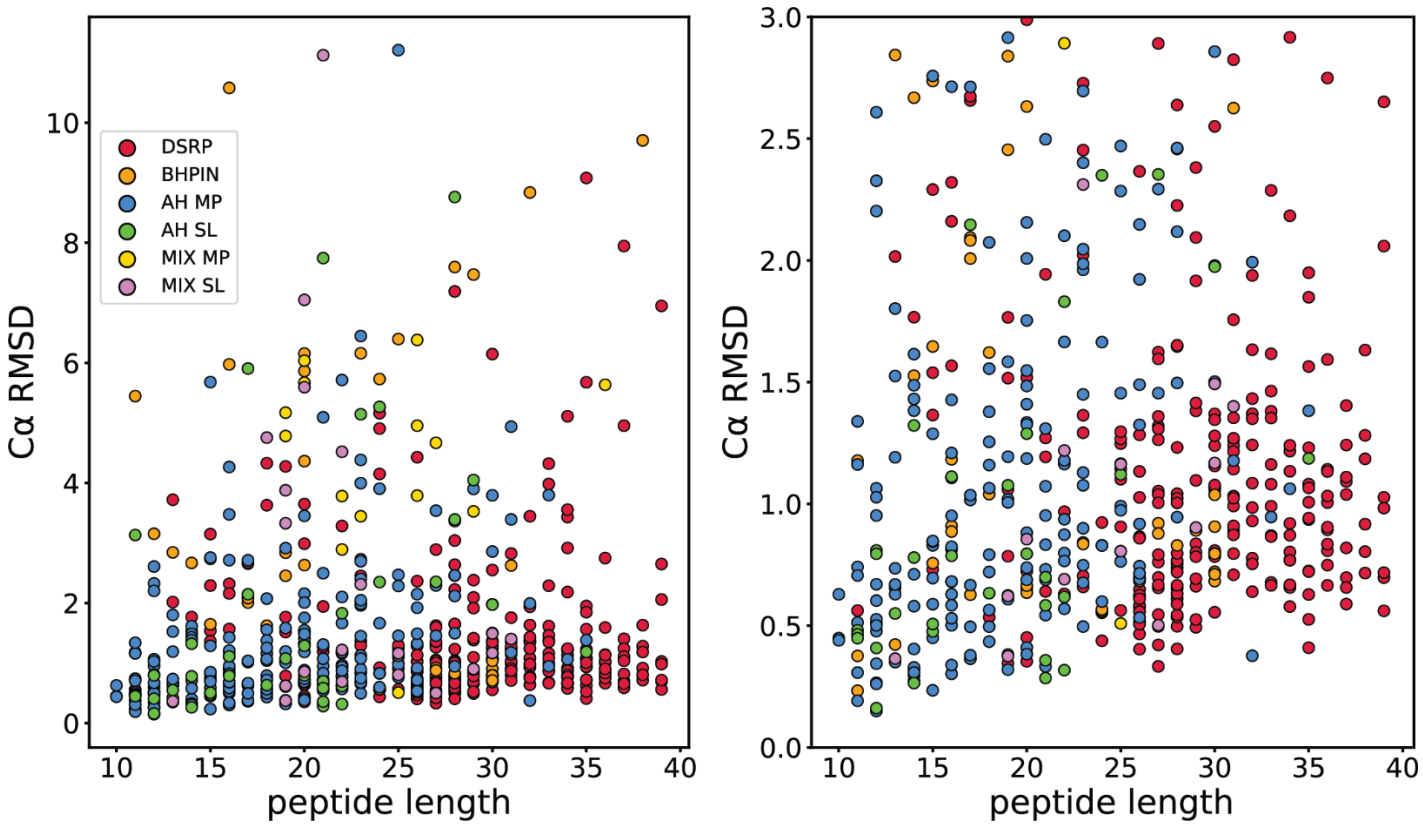

Supplementary Figure S6. AlphaFold2 predicted short peptides with higher accuracy than long peptides, Related to Figure 5. A. Scatter plot of Cα RMSD versus peptide length demonstrates a positive trend, which increasing Cα RMSD for longer peptides. Point color coded by peptide type with DSRPs in red, BHPINs in orange, AH MP in blue, AH SL in green, MIX MP in yellow, and MIX SL in purple. Note, DSRPs showed the least correlation and make up most long length peptides. These peptides also have more contacts and thus AF2 was better at folding them because MSAs provided structural information, unlike for the more unstructured peptide classed considered in this study. **B.** The same scatter plot with the y axis adjusted from 1.0 to 3.0 Å for clear viewing of low Cα RMSD range.

Supplemental Tables

Supplemental Table 2, in relation to Figure 4: List of all the DSRP disulfide connectivity patterns as identified in experimental structures versus AF2-predicted structures, along with information on whether the particular peptide was identified as an RMSD outlier.

NMR disulfide bond pattern		AF2 disulfide bond pattern		RMSD outliers?
1EWS				
3	29	3	28	n
5	12	5	19	
9	28	9	29	
1G26				
4	16	4	26	n
10	26	10	16	
1IM1				
2	18	3	12	n
3	12	-	-	
1K0P				
2	28	7	28	n
7	25	-	-	
1M4E				
2	18	2	18	n
5	17	5	8	
6	14	6	14	
8	9	9	17	
1M4F				
7	23	7	23	y
10	22	10	12	
11	19	11	19	
13	14	13	22	
1N5G				
4	30	4	27	y
9	27	9	30	
1S6W				
2	19	2	19	n
5	18	5	8	
6	15	6	15	
8	9	9	18	

1TYK				
2	17	2	16	n
9	23	9	9	
16	30	17	30	
2B5B				
4	30	4	29	y
8	29	8	24	
12	24	12	30	
2BBG				
5	35	5	18	y
11	26	11	28	
18	28	19	39	
19	39	-	-	
2DDL				
3	23	3	23	n
8	28	8	28	
12	30	12	30	
18	33	-	-	
2L1J				
1	16	1	16	n
8	15	8	22	
24	31	15	33	
		24	31	
2MIX				
4	20	4	21	y
5	21	7	16	
7	16	-	-	
2MM5				
1	16	1	16	n
8	15	8	21	
		15	29	
2MSF				
4	12	4	21	y
7	28	7	26	
11	21	11	28	
16	26	-	-	
3BBG				
5	35	5	11	y
11	26	18	26	

18	28	19	39	
19	39			
6NUG				
1	13	1	13	n
7	23	7	23	
14	24	-	-	
6NW8				
2	23	12	23	y
5	18			
12	25			
7ELY				
2	25			y
12	26	12	28	
14	20			
7L7A				
2	9	-	-	y
3	11	-	-	

Supplemental Table 3, in relation to Star Methods: The PDB IDs, range of the structured regions, length and sequence information, and the description of the peptides used for the comparison of NMR and X-ray structures that have identical ordered regions.

NMR PDB ID	Xray PDB IB	Type	Structured Region for RMSD calculation	NMR FASTA Sequence	Xray FASTA sequence	Length	Description
2UVS	3ODV	DSRP	1-38	GVEINVKCSGSPQCLKPCKDAGMRFGKCMNRKCHCTPK	GVEINVKCSGSPQCLKPCKDAGMRFGKCMNRKCHCTPK	38	High Resolution Solid-state NMR structure of Kaliotoxin
1E4Q	1FD3	DSRP	28-64	PVTCLKSGAICHPVFCPRRYKQIGTCGLPGTKCCKKP	GIGDPVTCLKSGAICHPVFCPRRYKQIGTCGLPGTKCCKKP	37	Solution structure of the human defensin hBD-2
1E4S	1IJU	DSRP	33-68	DHYNCVSSGGQCLYSACPIFTKIQGTCYRGKAKCCK	DHYNCVSSGGQCLYSACPIFTKIQGTCYRGKAKCCK	36	Solution structure of the human defensin hBD-1
1ERC	6E6O	DSRP	1-40	DACEQAAIQCVESACESLCTEGEDRTGCYMYIYSNCPPYV	DACEQAAIQCVESACESLCTEGEDRTGCYMYIYSNCPPYV	40	THE NMR SOLUTION STRUCTURE OF THE PHEROMONE ER-1 FROM THE CILIATED PROTOZOAN EUPLOTES RAIKOVI
1Q2K	3E8Y	DSRP	1-31	AACYSSDCRVKCVAMGFSSGKCINSKCKCYK	AACYSSDCRVKCVAMGFSSGKCINSKCKCYK	31	Solution structure of BmBKTx1 a new potassium channel blocker from the Chinese Scorpion Buthus martensi Karsch

1ROO	4LFQ	DSRP	3-35	RSCIDTIPKSRCTAFQCKHSMKYRLSFCRKTCGTC	RSCIDTIPKSRCTAFQCKHSMKYRLSFCRKTCGTC	35	NMR SOLUTION STRUCTURE OF SHK TOXIN, NMR, 20 STRUCTURES
1TSK	6ATL	DSRP	1-35	VVIGQRCYRSPDCYSACKKLVGKATGKCTNGRCDC	GSVVIGQRCYRSPDCYSACKKLVGKATGKCTNGRCDC	35	SCORPION TOXIN (TS KAPPA) FROM TITYUS SERRULATUS ACTIVE ON SMALL CONDUCTANCE POTASSIUM CHANNEL, NMR, 30 STRUCTURES
1V6R	6DK5	DSRP	1-21	CSCSSLMDKECVYFCHLDIIW	CSCSSLMDKECVYFCHLDIIW	21	Solution Structure of Endothelin-1 with its C-terminal Folding
1ZFU	3E7R	DSRP	4-40	GFGCNGPWDEDDMQCHNHCKSIKGYKGGYCAKGGFVCKCY	GFGCNGPWDEDDMQCHNHCKSIKGYKGGYCAKGGFVCKCY	40	Plectasin:A peptide antibiotic with therapeutic potential from a saprophytic fungus
2KHB	4TTM	DSRP	4-28	GLPVCGETCVGGTCNTPGCTCSWPVCTRN	GLPVCGETCVGGTCNTPGCTCSWPVCTRN	29	Solution structure of linear kalata B1 (loop 6)
2KTX	3ODV	DSRP	3-38	GVEINVKCSGSPQCLKPCKDAGMRFGKCMNRKCHCTPK	GVEINVKCSGSPQCLKPCKDAGMRFGKCMNRKCHCTPK	38	COMPLETE KALIOTOXIN FROM ANDROCTONUS MAURETANICUS MAURETANICUS, NMR, 18 STRUCTURES
2LXZ	1ZMP	DSRP	1-32	ATCYCRTGRCATRESLSGVCEISGRLYRLCCR	ATCYCRTGRCATRESLSGVCEISGRLYRLCCR	32	Solution Structure of the Antimicrobial Peptide Human Defensin 5
2MAU	4BFH	DSRP	1-30	CAQKGEYCSVYLQCCDPYHCTQPVIGGICA	CAQKGEYCSVYLQCCDPYHCTQPVIGGICA	30	Solution structure of alpha-amylase inhibitor wrightide R1

							(wR1) peptide from Wrightia religiosa
2N9T	5O0U	DSRP	1-28	YCQKWMWTCDSERKCCEGMVCRLWCKKKLW	YCQKWMWTCDSERKCCEGMVCRLWCKKKLW	30	NMR solution structure of ProTx-II
2V1V	1LU0	DSRP	2-29	RVCPRILLECKKDSDCLAECVCLEHGYCG	RVCPRILLECKKDSDCLAECVCLEHGYCG	29	3D STRUCTURE OF THE M8L MUTANT OF SQUASH TRYPSIN INHIBITOR CMTI-I
5L1C	6ATW	DSRP	1-36	MCMPCFTTDHQMARKCDDCCGGKGRGKCYGPQCLCR	GSMCMPCFTTDHQMARKCDDCCGGKGRGKCYGPQCLCR	36	Heteronuclear Solution Structure of Chlorotoxin